Stripline-Based W-Band Frequency Scanning Composite Right/Left-Handed Leaky-Wave Antenna with a Tapered Aperture for Narrow Beamwidth

Zhi Li[#1], Nathan Chordas-Ewell[#], Jun H. Choi[#2], Dongyin Ren[$3], Ryan Wu[$], Zeeshan Qamar[*], Nafati Aboserwal[*], Jorge L. Salazar-Cerreno[*4]

[#]Department of Electrical Engineering, The State University of New York at Buffalo, Buffalo, NY, USA
[$]NXP Semiconductors, San Jose, CA, USA
[*]Advanced Radar Research Center (ARRC), The University of Oklahoma, Norman, OK, USA
[1]zli76@buffalo.edu, [2]junhchoi@buffalo.edu, [3]dongyin.ren@nxp.com, [4]salazar@ou.edu

2021 IEEE/MTT-S International Microwave Symposium - IMS 2021 | 978-1-6654-0307-8/21/$31.00 ©2021 IEEE | DOI: 10.1109/IMS19712.2021.9574871

***Abstract*— A stripline-based composite right/left-handed (CRLH) leaky-wave antenna (LWA) with a tapered aperture is designed for an increased effective aperture size. Experimental results show that the CRLH LWA is able to scan from -33° to 25.5° by sweeping the frequency from 76.75 GHz to 83 GHz, with a half-power beamwidth (HPBW) of less than 5°.**

***Keywords*— stripline, leaky-wave antennas, composite right/left-handed transmission lines, W-band, tapered aperture.**

I. Introduction

Leaky-wave antennas (LWAs) can provide beam steering through frequency scanning as a practical solution for high-frequency applications. For the realization of LWAs in the W-band, waveguides or substrate integrated waveguides (SIWs) are commonly used as the host structure, through which the leaky wave propagates [1]–[5]. A meandered SIW with slots shows a wide scanning range from backward to forward using a narrow operating freuqency band and demonstrates a narrow half-power beamwidth (HPBW) [1]. The rectangular waveguide realization in [2] provides similar features. However, these structures are not suitable for 2D arrays due to their wide dimensions in the transverse direction, thus prohibiting formation of pencil-beam radiation. A rectangular groove filled with air or dielectric is adopted in [3] and [4]. By filling the groove with dielectric and modulating the groove depth, wide beam-scanning through broadside is achieved [3]. In [4], the air-filled groove is loaded with a slotted metal sheet on top to enable forward beam scanning. Both designs have limited dispersion and require wide operating frequency bands to achieve the desired scanning range. The design of a substrate integrated image guide with a grating of metal strips placed on its top surface provides better dispersion, but can only scan in the forward region [5]. None of the above solutions satisfy all four requirements of compact size, high dispersion, forward-to-backward scanning, and narrow beamwidth, which are preferred in certain W-band radar applications.

Composite right/left-handed (CRLH) transmission line (TL) based LWAs seem to be a good candidate for the aforementioned requirements. The dispersion of CRLH LWAs can be easily engineered to achieve desired phase variation over a relatively narrow operating frequency band, resulting in a wide scanning range including broadside radiation. Once the 1D CRLH LWA is designed, the 2D array can be formed by arranging multiple 1D antennas in the transverse dimension. In [6], a stripline-based CRLH LWA is proposed, which in simulation shows backward-to-forward scanning using the frequency band from 76 GHz to 81 GHz. The simulated HPBW ranges from 6° to 9°. However, the effective aperture size of the antenna shown in [6] cannot be further increased due to the very low field intensity towards the end of the antenna. Both the reduction of material loss and the manipulation of the current amplitude distribution can help elongate the effective aperture of LWAs. This paper builds on [6], with the efforts made to increase the effective aperture size by applying a sectionally tapered aperture.

In Section II, descriptions will be given regarding the unit-cell and the CRLH LWA with a tapered aperture. Measured results are discussed in Section III, with comparison to the full-wave simulation results.

II. Antenna Descriptions

The unit-cell design is shown in Fig. 1 [6]. The presented CRLH LWA is composed of 75 unit-cells, which lead to a physical aperture length of $100\,\mathrm{mm}$. Without affecting the dispersion, radiation efficiency of each unit-cell can be increased by increasing the slot offset x indicated in Fig. 1 from $0.12\,\mathrm{mm}$ to $0.42\,\mathrm{mm}$. Ideally, the taper would be designed with the radiating slot of each unit-cell tuned so that leakage constant increases continuously along the aperture to compensate for the exponentially decaying current amplitude distribution. However, such approach leads to a more complex design that requires each unit-cell to match a specific efficiency value while maintaining the same dispersion. Instead, a quasi-uniform current amplitude distribution over the aperture is realized by cascading multiple sections of unit-cells in the antenna, with each section bearing a different yet precisely controlled efficiency value.

Let the number of sections be M, the number of unit-cells in each section be N_m, and the radiated power of an arbitrary cell in this antenna be $P_{r(m,n)}$, where

$$m = \{1, 2, 3, \ldots, M\}, n = \{1, 2, 3, \ldots, N_m\},$$

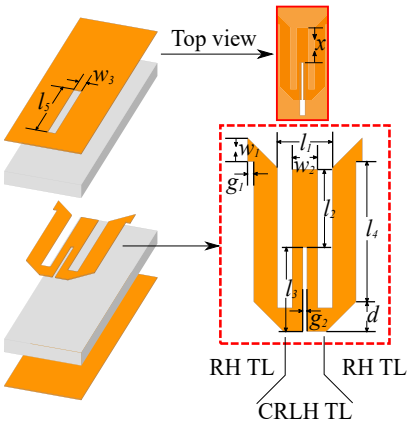

Fig. 1. Unit-cell of the 1D CRLH LWA: $w_1 = 0.275\,\text{mm}$, $w_2 = 0.3\,\text{mm}$, $w_3 = 0.14\,\text{mm}$, $l_1 = 0.65\,\text{mm}$, $l_2 = 0.92\,\text{mm}$, $l_3 = 0.9875\,\text{mm}$, $l_4 = 1.65\,\text{mm}$, $l_5 = 1.4\,\text{mm}$, $g_1 = 0.075\,\text{mm}$, $g_2 = 0.05\,\text{mm}$, $d = 0.35\,\text{mm}$. Orange parts are copper with thickness of 17.5 um, and gray parts are Rogers RO3003 laminates with thickness of 10 mil.

$$\sum_{m=1}^{M} N_m = \frac{L}{p}, \tag{1}$$

and L is the total antenna length, and p is the period of the unit-cell. For example, if $m = 1, n = 2$, then $P_{r(1,2)}$ is the radiated power of the second cell in the first section. We obtain an equation that relates the radiated power of an arbitrary cell $P_{r(m,n)}$ to its total attenuation constant $\alpha_{t(m)}$ (radiation + material loss) and its attenuation constant due to radiation $\alpha_{r(m)}$:

$$P_{r(m,n)} = 2P_0\left\{e^{-2p\sum_{k=1}^{m-1} N_k\alpha_{t(k)}}\right\}\{e^{-(2n-1)\alpha_{t(m)}p}\}\sinh(\alpha_{r(m)}p), \tag{2}$$

where P_0 is the input power. The term in the first curly brackets denotes the attenuation experienced in the previous $(m-1)$ sections. The term $2\{e^{-(2n-1)\alpha_{t(m)}p}\}\sinh(\alpha_{r(m)}p)$ can be understood in the following way. The attenuation undertaken in the *m*th section before the *n*th cell is $e^{-2(n-1)\alpha_{t(m)}p}$. In the *n*th cell depicted by Fig. 2, the power undergoes the material loss of a half unit-cell, which contributes to an attenuation of $e^{-(\alpha_{t(m)}-\alpha_{r(m)})p}$. Then the cell radiates by the amount of $1 - e^{-2\alpha_{r(m)}p}$. Multiplying the three terms above and factoring out $e^{-\alpha_{r(m)}p}$ gives the exact term of $2\{e^{-(2n-1)\alpha_{t(m)}p}\}\sinh(\alpha_{r(m)}p)$.

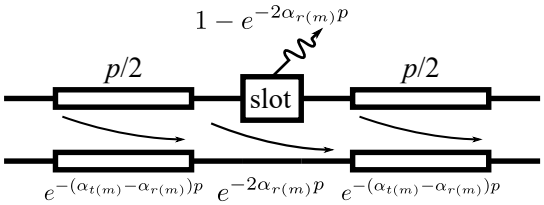

Fig. 2. Loss in a unit-cell.

In order to find $P_{r(m,n)}$, there are $m+1$ unknowns to solve for: the total attenuation constant of each of the m sections and the attenuation constant due to radiation in the *m*th section. Notice that by setting $m = 1$, the summation of (2) over n returns the total radiated power of the *m*th section when the section stands alone, which can be extracted from simulating a shorter antenna of 15 unit-cells belonging to that section. $\alpha_{t(m)}$ can also be calculated from the same simulation using insertion loss data. Then we can solve for $\alpha_{r(m)}$. By simulating each of the m sections, all the unknowns are obtained. Therefore, $P_{r(m,n)}$ can be calculated for any antenna layout configuration controlled by M, N_m, and $\alpha_{r(m)}$.

Once the radiated power of all cells for a given antenna is calculated, it is simpler to approximate the corresponding current distribution, which can be used to calculate array factors (AFs). Without fundamentally reducing the material loss, the application of a taper can be treated as an optimization problem about achieving the narrowest beamwidth while maintaining a relatively high gain. The approximation of a current distribution can provide a faster estimation of the shape of the beam compared to full-wave simulation.

Using this method, a tapered aperture is designed by cascading 4 sections of unit-cells. The values of slot offset x for each section starting from the input are $0.22\,\text{mm}$, $0.24\,\text{mm}$, $0.28\,\text{mm}$, and $0.34\,\text{mm}$, and numbers of unit-cells in these sections are 4, 9, 11, and 51, respectively.

III. Experimental Results

Fig. 3 shows the fabricated CRLH LWA. Grounded coplanar waveguide (GCPW) is used as an intermediate stage to transit from coax to stripline. In order to reduce the likelihood of breakage from the lack of rigidity in the substrate, a 3D printed backing made of PLA ($\epsilon_r \approx 3.2$, $\tan\delta \approx 0.03$) is designed and affixed to the back of the antenna. The back of the antenna is taped to the PLA backing so that no tape is near the radiating slots, and a copper shield is placed over the transition region to minimize radiation interference from the transition.

Normalized E-plane radiation patterns are measured from 76.75 GHz to 83 GHz with a 0.25 GHz step. Fig. 4 shows the patterns at 6 different frequencies along with the simulated results. A measured dielectric constant of $\epsilon_r = 2.91$ for Rogers RO3003 [7] is used in our simulation. Except for the small difference in scanning angle at lower frequencies, the measured results agree well with simulated data. From 76.75 GHz to 83 GHz, a scanning from $-33°$ to $25.5°$ is achieved. A HPBW of

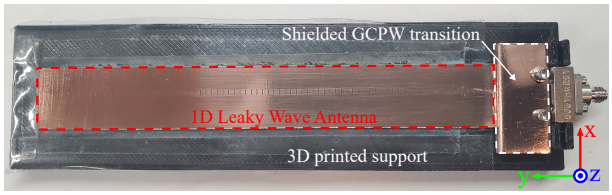

Fig. 3. Assembled CRLH LWA with a connectorized transition, a shield, and a backing structure.

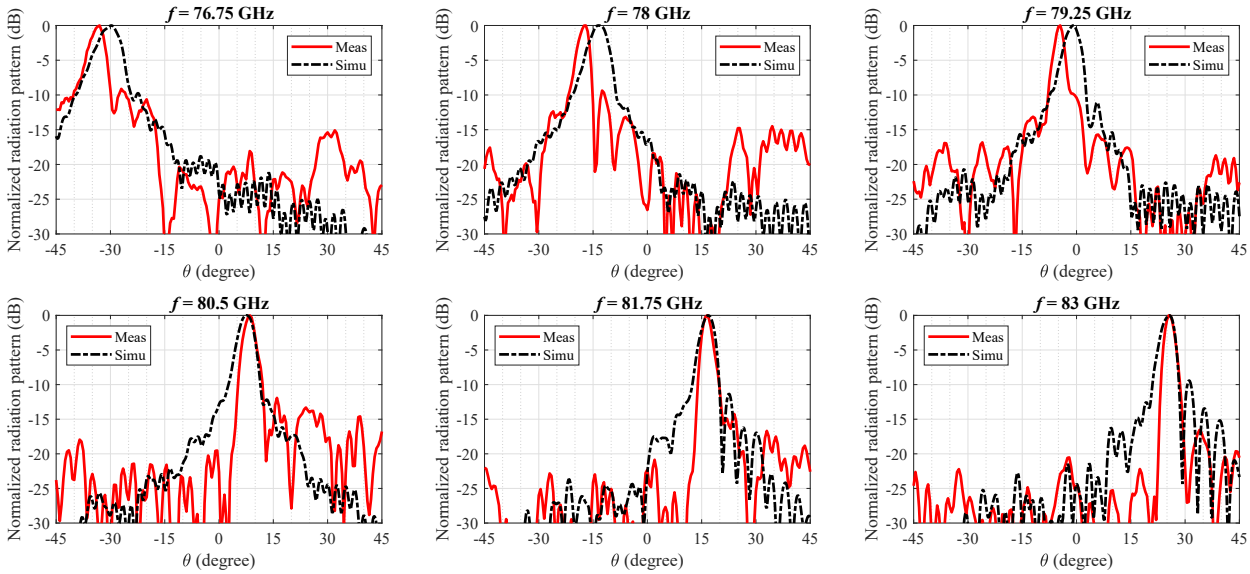

Fig. 4. Measured and simulated normalized radiation patterns in E-plane ($\phi = 90°$) of the CRLH LWA with a connectorized transition at different frequencies.

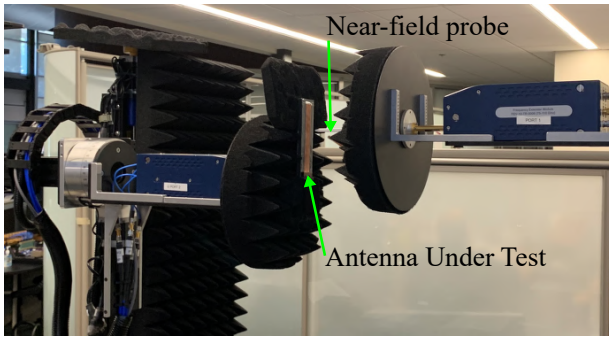

Fig. 5. Near-field measurement setup for the CRLH LWA with a connectorized transition.

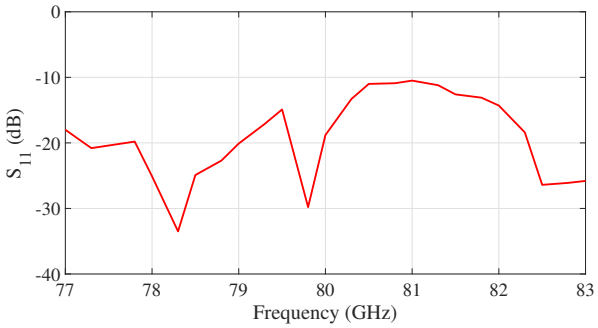

Fig. 6. Measured S_{11} of the CRLH LWA with a connectorized transition and a waveguide adapter.

less than $5°$ is observed even in the worst case at 76.75 GHz. Measured gain is not available due to measurement constraints, however the simulated gain is 14 dBi at 80.75 GHz. The near-field setup used in this measurement is shown in Fig. 5. Fig. 6 shows the measured S_{11}, which is calibrated up to the input of the waveguide-to-coax adapter.

IV. Conclusion

In this paper, a sectionally tapered aperture designed by a fast approximation method for beam shape prediction is successfully applied to increase the effective aperture size of the stripline-based CRLH LWA. Measurement results of the fabricated antenna verify the design concept. This antenna provides a low-cost solution to the simultaneous requirements of compact size, backward-to-forward scanning, high dispersion, and narrow beamwidth. With further investigation into the reduction of material loss, this type of antenna may be able to achieve even larger effective aperture sizes.

References

[1] N. Wang and L. Wang, "A frequency beam scanning substrate integrated waveguide slot array antenna for 94 GHz band," in *IEEE Int. Symp. Antennas Propag. (APSURSI)*, 2016, pp. 797–798.

[2] T. Bernabeu-Jiménez, X. Begaud, F. Magne, M. Hadjloum, and B. Cosson, "Snaky leaky wave antenna for scanning applications in w band," in *2018 IEEE Conf. Antenna Meas. Appl. (CAMA)*, 2018, pp. 1–4.

[3] X. Bai, S. Qu, K. Ng, and C. H. Chan, "Sinusoidally modulated leaky-wave antenna for millimeter-wave application," *IEEE Trans. Antennas Propag.*, vol. 64, no. 3, pp. 849–855, 2016.

[4] D. A. Schneider, M. Rösch, A. Tessmann, and T. Zwick, "A low-loss w-band frequency-scanning antenna for wideband multichannel radar applications," *IEEE Antennas Wireless Propag. Lett.*, vol. 18, no. 4, pp. 806–810, 2019.

[5] Y. J. Cheng, Y. X. Guo, X. Y. Bao, and K. B. Ng, "Millimeter-wave low temperature co-fired ceramic leaky-wave antenna and array based on the substrate integrated image guide technology," *IEEE Trans. Antennas Propag.*, vol. 62, no. 2, pp. 669–676, 2014.

[6] D. Ren, Z. Li, J. H. Choi, and R. Wu, "1D & 2D w-band frequency scanning metamaterial antenna and array," in *IEEE Int. Symp. Antenna Propag. (APSURSI)*, 2020, pp. 171–172.

[7] S. S. Jehangir, Z. Qamar, N. Aboserwal, and J. L. Salazar-Cerreno, "Application of the mixing theory in the design of a high-performance dielectric substrate for microwave and mm-wave systems," *IEEE Access*, vol. 8, pp. 180 855–180 868, 2020.